International Journal of Adhesion & Adhesives 138 (2025) 103934

Contents lists available at ScienceDirect

International Journal of Adhesion and Adhesives

journal homepage: www.elsevier.com/locate/ijadhadh

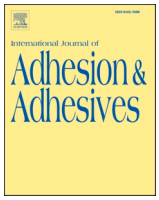

Enhanced adhesion properties of hyperelastic adhesives to different nature substrates by applying different surface treatments

Óscar Cuadrado-Sempere [a,*], Francisco-Javier Simón-Portillo [a], Carlos Ruzafa-Silvestre [b], Elena Orgiles-Calpena [b], Francisca Arán-Aís [b], Lucas Filipe Martins da Silva [c], Miguel Sánchez-Lozano [a]

[a] University Institute of Engineering Research of Elche, I3E. Miguel Hernández University, 03202, Elche, (Alicante), Spain
[b] INESCOP. Center for Innovation and Technology, 03600, Elda, (Alicante), Spain
[c] Department of Mechanical Engineering, Faculty of Engineering, University of Porto, Rua Dr. Roberto Frias, 4200-465, Porto, Portugal

ARTICLE INFO

Keywords:
Adhesive bonding
Surface treatment
Plasma
Contact angle
Bond strength

ABSTRACT

This study investigates the effect of different surface treatments on the bond strength of hyperelastic adhesive joints. Plasma treatment and primer application were compared to sandblasting and sandblasting plus priming on aluminium and Glass-fibre Reinforced Polyester (GRP) surfaces. Results indicated that plasma treatment on aluminium surfaces increased shear strength values by 20 % compared to untreated surfaces and showed a shear strength comparable to primer application. However, on GRP surfaces, primer application improved bond strength by 10 %, while plasma treatment did not provide any significant enhancement. Plasma and primer treatments produce predominantly cohesive joint failure, while sandblasting and sandblasting plus priming produce large percentage of adhesive failure. Plasma treatment may serve as a good alternative to primer on aluminium surfaces, while primer remains preferred for GRP surfaces. The study concludes that the dispersive contact angle has a direct relationship with shear strength, where a 50 % decrease in dispersive contact angle results in a 10 % increase in shear strength. This suggests that substrate surfaces with a higher affinity for dispersive compounds would form stronger bonds.

1. Introduction

In recent years, the aerospace and automotive industries have widely adopted lightweight materials and composites due to their excellent stiffness-to-weight and strength-to-weight ratios. Achieving the lightest possible bond is the ultimate goal [1–6].

Single-component polyurethane (PU) adhesives are commonly used when high bond strength and flexibility are required [7]. Industrial and academic advancements are being directed towards creating more sustainable solutions by reducing the environmental impact of isocyanates and developing isocyanate-free polyurethanes [8]. However, the use adhesives based on Silane-Modified Polymers (SMP) is increasing due to concerns regarding the use of isocyanates in polyurethane synthesis [9]. These are non-isocyanate compounds, more environmentally friendly [10–12]. Different authors agree that they could be a good alternative to PU adhesives [7–9,13,14].

Both PU and SMP adhesives possess characteristics such as high expansion and contraction, good sealing properties, and the ability to join various metals (steel, aluminium), plastics (ABS, PVC, PP), glass, and composite materials, including reinforced glass, fibre-reinforced plastics, and Glass-fibre Reinforced Polyester (GRP) panels, among others. These adhesives can also withstand impacts, high vibrations, and high resistance to tear propagation, providing a high safety coefficient. This enables the detection of damaged joints and the preventive repair of the joints before they break.

These adhesives are characterized by their elastic behaviour with large deformations, similar to rubbers or elastomers, reaching elongations of more than 200 %. In addition, they exhibit a non-linear load-deformation relationship, which makes their behaviour more closely resemble that of a hyperelastic material [15–17]. An advantage of these high-elongation adhesives is their ability to reduce stress in the final joints and mitigate the transmission of vibrations [2,3]. Moreover,

* Corresponding author.
E-mail addresses: ocuadrado@umh.es (Ó. Cuadrado-Sempere), f.simon@umh.es (F.-J. Simón-Portillo), cruzafa@inescop.es (C. Ruzafa-Silvestre), eorgiles@inescop.es (E. Orgiles-Calpena), aran@inescop.es (F. Arán-Aís), lucas@fe.up.pt (L.F. Martins da Silva), msanchez@umh.es (M. Sánchez-Lozano).

https://doi.org/10.1016/j.ijadhadh.2025.103934
Received 4 July 2023; Received in revised form 16 December 2024; Accepted 2 January 2025
Available online 4 January 2025

depending on the substrate material and the surface treatment applied, the strength behaviour of the joint can vary. There are various studies on possible surface treatments and how they can affect the joint [4,5, 18–25]. Most of the literature found using aluminium or GRP focuses on the mechanical characteristics of the joint with epoxy adhesives, while fewer studies [26] have examined the use of hyperelastic PU in such studies.

Hyperelastic structural adhesives have numerous advantages, but their application has been limited due to the paucity of information on their behaviour in structural joints. Therefore, it is essential to investigate the behaviour of these adhesives and bonds in service conditions. Furthermore, since these adhesives are widely used, it is necessary to investigate their application conditions, particularly when used in structural applications such as the production of lightweight vehicles.

The objective of this research was to analyse the sensitivity of the mechanical characteristics of the bond to the variation of different adhesive application parameters, including possible surface treatments of the materials to be bonded, in order to determine the best application conditions. The study aimed to compare the strength of joints made with a hyperelastic SMP adhesive on different substrates treated with various surface treatments, including chemical treatments (priming), sandblasting, or plasma treatment.

Aluminium and glass fibre-reinforced polyester, which are commonly used in applications with relative structural responsibility and in lightweight vehicles, were the primary materials tested. The research aimed to guarantee the bond between materials and ensure that, in the event of bond failure, it would be due to a cohesive failure of the adhesive caused by complete exhaustion of the mechanical strength of the adhesive, which in turn guarantees the propagation of the breakage.

2. Methodology

The methodology used can be divided into four parts is divided into four parts, which were applied consecutively to each of the substrate materials used (aluminium and GRP). It is explained below (see also the flowchart in Fig. 1 for a better understanding, and Fig. 2 for see the experimental techniques and equipment used):

Phase 1. Surface treatments. The substrate surfaces were subjected to various treatments, including primer film application, sandblasting, and atmospheric plasma treatment. For the atmospheric plasma treatment, different application parameters were used to assess their sensitivity, which would be analysed in the subsequent phase.

Phase 2. Surface characterization. The surfaces were characterised both before and after the application of the different treatments. To determine the most effective surface treatment for each material, contact angle and surface roughness measurements were conducted. For atmospheric plasma treatments, the sensitivity to various plasma application parameters was analysed. After a preliminary analysis, only a few parameter sets—expected to give the best results in the next phase—were selected for roughness measurements.

Phase 3. Single Lap Joint (SLJ) tests. In view of the preliminary results obtained, a series of standardised specimens were made using the selected surface treatments, and were tested to determine the maximum shear strength and the type of failure obtained in the bond: adhesive or cohesive. The objective is to eliminate the possibility of adhesive failure, so that cohesive breaks are produced in the joint tests, and the maximum stress values supported by the adhesive in the different conditions can be

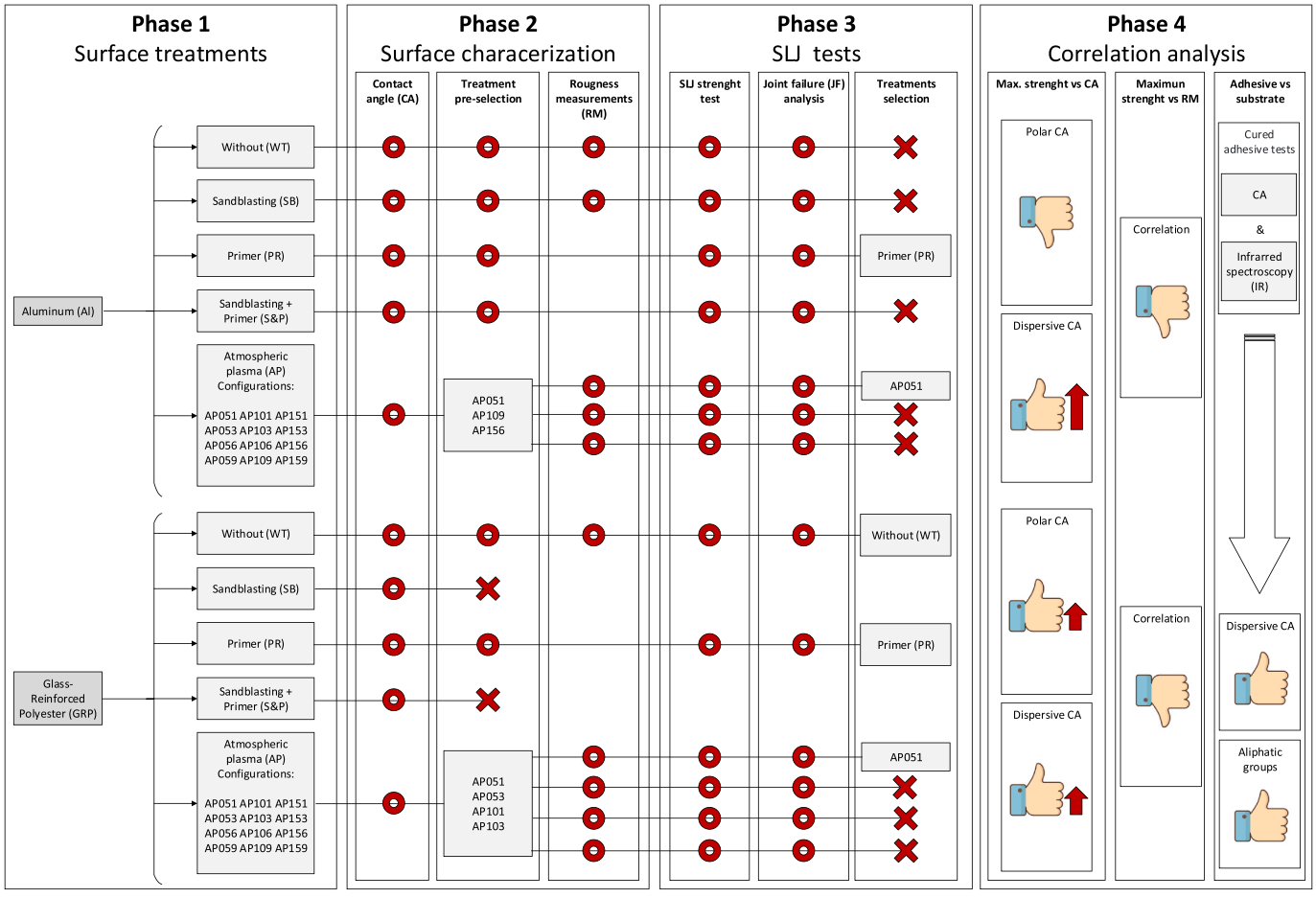

Fig. 1. Methodology diagram of the review.

Fig. 2. Experimental techniques and equipment.

analysed. This phase concludes with the selection of the most effective surface treatments, those that demonstrated improvements in shear strength.

Phase 4. Correlation analysis. Finally, correlations were explored between the surface characteristics obtained in Phase 2 and the shear strengths of the adhesive bonds measured experimentally in Phase 3. Additional tests were conducted on specimens of cured raw adhesive material, to search for affinities between the adhesive and the substrate surfaces. This phase concludes with the analysis of affinities between the surface properties, adhesive and bond performance.

All treatments and tests were conducted at the INESCOP® Innovation and Technology Center testing laboratory, which is accredited by the National Accreditation and Certification Body (ENAC®) as a testing laboratory according to ISO 17025 and ISO 9001 quality standards. The testing room maintained a constant temperature of 25° ± 1° and a relative humidity between 50 ÷ 53 %.

3. Materials

Magnesium-aluminium alloy (EN AW-5754) and Glass-fibre Reinforced Polyester were used as substrates. For the primary bonding of SLJ specimens, Henkel Teroson® MS 939 (Henkel Ibérica, S.A., Spain) was used, which is a high-strength, moisture-curing adhesive SMP. To stiffen the main body of the specimens, cold-drawn S275JR structural steel plates were bonded to the main substrates using Araldite Standard® (CEYS, Spain) two-component epoxy adhesive, which has a very high shear strength. See Table 1 for material properties.

4. Surface Treatments

The chosen surface treatments are detailed below and the equipment used could be seen on Fig. 2. The application of some of the recommendations in standard EN 13887:2013 was contemplated. For a better understanding of the results in the following sections, the coding shown

Table 1
Material properties of the adherend and adhesives.

	Steel (S275JR)	Magnesium-aluminium alloy (EN AW-5754)	Fibre-reinforced polyester (GRP)	Henkel Teroson® MS 939	Araldite Standard®
Young's modulus, E (MPa)	210000	68900	2000	7	2000
Yield shear strength, fy (MPa)	275	240	58	3	22 ÷ 24
Density, ρ (g/cm^3)	7.8	2.7	1,3	1,5	1,1
Elongation, %	22	2	3 ÷ 5	250	1 ÷ 10
Thermal conductivity, λ (W/(m K))	40 ÷ 45	180	0,4	–	–

in Table 2 will be used to designate each of the treatments.

4.1. Mechanical treatment. Sandblasting

The sandblasting treatment was applied using a BT Ingenieros® compressed air sandblasting cabin, model CBCH90, with a working pressure up to 6.2 bar and air flow of 340 l/min. Brown corundum sand with a grain size of 46 was used. The pressure was set to 6 bar, and the sandblasting time was 15 s, with a nozzle-to-surface distance of approximately 20 mm. After the sandblasting, the surfaces were cleaned with pressurised air to remove any loose particles and debris.

4.2. Chemical treatment. Primer film

The chemical primer treatment selected was Teroson® PU 8511 (Henkel Ibérica, S.A., Spain), a solvent-based PU solution primer, commonly used to improve the adhesion of PU-based one-component adhesives. Although the adhesive manufacturer does not recommend the use of a primer for aluminium or GPR surfaces, previous studies by our group [27] and other authors [18–20] found that using this primer prevented adhesive breakage. Without the primer, breakage was completely cohesive.

The primer was applied using a sponge. The primer was allowed to dry for 20 min at INESCOP® laboratory room temperature before further treatments were applied.

4.3. Chemical treatment. Cold atmospheric plasma

A Diener Electronic® cold air current atmospheric plasma equipment, model PlasmaBeam Standard (Diener Electronic Gmbh & Co, Germany), was used for chemical plasma treatment. The equipment operates at room temperature, 20 kHz and 20 kV discharge voltage and has a 6 mm diameter cylindrical nozzle, which produces a flow at 6 bar pressure. The equipment is also equipped with a robotic arm that allows the height and speed of the nozzle to be adjusted.

Prior to application, the surfaces were allowed to cool to the aforementioned ambient test temperature laboratory. The treatment time was 30 s, and the nozzle-to-surface distance (d_a), mm and speed of the nozzle (v_p) was adjusted to 5, 10 and 15 mm and 1, 3, 6 and 9 cm/s, respectively. This makes a total of 12 possible combinations of parameters.

Table 2
Treatments codification and references.

Treatments		Ref. Aluminium	Ref. GRP
Without (WT)		WT-AL	WT-G
Sandblasting (SB)		SB-AL	SB-G
First (PR)		PR-AL	PR-G
Sandblasting + Primer (S&P)		S&P-AL	S&P -G
Atmospheric plasma configurations (AP)			
Distance (d_a), mm	Velocity (v_p), m/s		
5	0,01	AP051-AL	AP051-G
	0,03	AP053-AL	AP053-G
	0,06	AP056-AL	AP056-G
	0,09	AP059-AL	AP059-G
10	0,01	AP101-AL	AP101-G
	0,03	AP103-AL	AP103-G
	0,06	AP106-AL	AP106-G
	0,09	AP109-AL	AP109-G
15	0,01	AP151-AL	AP151-G
	0,03	AP153-AL	AP153-G
	0,06	AP156-AL	AP156-G
	0,09	AP159-AL	AP159-G

5. Experimental techniques

5.1. Contact angle measurements

Surface energy of the untreated and treated surface adherents were evaluated by means of contact angle measurements according to the procedure described in the DIN 828 standard and the Owens-Wendt method [28]. For this purpose, a goniometer made by MUVER (Elda, Spain) was used. The equipment has a thermostatised chamber, which allows working in a saturated atmosphere, with an exhaustive control of the temperature at 25 °C. It is also provided with a vision system based on a camera with a telecentric lens, which is backlit by a matrix of LEDs. For each treated and untreated adherent, two samples were analysed using 3 drops (4 ml of volume) of two different standard liquids. As a polar one, deionised water (Millipore Elix system) was used to determine the average contact angle value. Furthermore, as a dispersive one, diiodomethane for synthesis (Sigma Aldrich, Germany) was used.

It is known that the polarity of the liquid can significantly influence the contact angles [28–32], that can be an indicator of the polar affinity of the material surface. These studies determined chemical affinities between adhesives and substrates based on total surface free energy. To obtain this energy, the contact angles with different liquids applied to the substrate surfaces were obtained. A low contact angle for all liquids used implies a higher surface free energy. This favours permeability, wettability, and, in turn, bond strength between adhesive and substrate.

Following these examples, contact angles with distilled water (polar liquid, θ_w) and diiodomethane (dispersive liquid, θ_d) were measured. With these angles and the literature consulted, the total free surface energy (γ_S) was calculated as the sum of the polar (γ_S^p) and dispersive (γ_S^d) components, using the Owen-Wendt method [26].

The contact angle measurements for aluminium, GRP, and cured adhesive were conducted using four specimens of each type. Each specimen used for the characterisation had dimensions of 30 x 30 x 3 mm.

Based on the literature [28–32], we could classify the relationship between contact angle and surface free energy as follows: angles $<10°$ correspond to very high surface free energies, $<30°$ high, $30° \div 90°$ medium and $>90°$ low or zero. In this study, a value of less than 30° was established as the average reference value for low angles or high energies.

5.2. Rugosimeter measurements

To determine the roughness of the surfaces, a Taylor Hobson SURTRONIC DUO roughness tester was employed to obtain the arithmetic mean roughness (R_a) and the maximum mean roughness (R_z) in accordance with ISO 4287:1999. The measurements adhered to the recommendations of the EN 10049:2013 standard.

Results obtained from some studies, such as [30], suggest a correlation of the polar components of the free surface energy and the contact angle with the arithmetic mean roughness, but their primary conclusion is the correlation of the dispersive components of the angle and the free surface energy with the maximum peak height roughness (R_p).

One specimen of each type was used for the measurements of R_a and R_z. The aluminium specimens measured 25 x 70 x 3 mm, while the GRP specimens measured 25 x 70 x 2 mm. To verify the uniformity of the surface treatment, ten measurements were taken in different areas along three distinct directions on the same surface, and the standard deviations of all measurements were evaluated. All measurements were conducted under the previously mentioned ambient testing conditions at the INESCOP® laboratory.

5.3. Chemical characterisation

A Varian 660-IR infrared spectrophotometer (Varian Australia PTY

LTD; Mulgrave, Australia) was used for the chemical characterisation of the adhesive film sample. Attenuated Total Reflection (ATR) technique was employed to perform 16 scans at a resolution of 4 cm^{-1}. A cured SMP adhesive sample with dimensions of 5 x 5 x 3 mm was utilised for infrared spectroscopy analysis.

5.4. Strength test and specimens

To determine the maximum tensile shear strength, single lap joints (SLJ) were created following EN 1465:2009 and tested on an Instron® 3366 universal testing machine (Instron®, Spain). The type of breakage was determined in accordance with ISO 10365:1996. The procedure established in EN 1465:2009 was followed to ensure the repeatability of the tests, which states that the difference between any two forces obtained from the same joint configuration, by the same operator, in the same laboratory, and using the same equipment should be less than 2.5 times the standard deviation.

The specimens were made using the same materials on both sides. As the adhesive is highly elastic and the primary mechanical strength value sought is the tensile shear strength, the bending peeling stress of the specimen was attempted to be suppressed by increasing the thickness of the substrate, as recommended by the standard. Steel plates were bonded to the specimens using Araldite Standard® two-component epoxy adhesive to provide them with greater rigidity. This adhesive

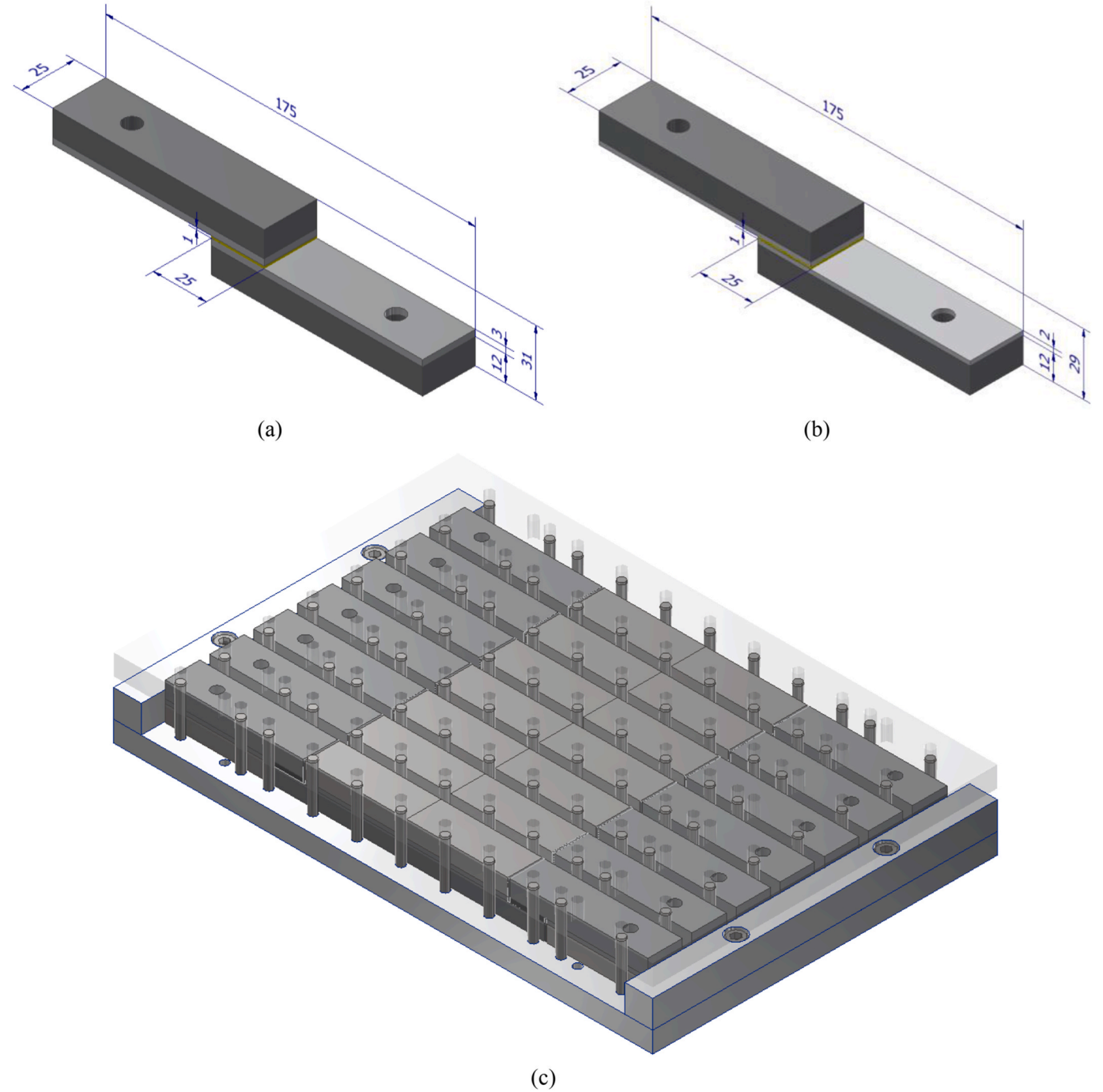

Fig. 3. Example of specimen configuration: a) Steel-Araldite Standard-Aluminium-Teroson® MS 939-Aluminium-Araldite Standard-Steel; b) Steel-Araldite Standard-GRP-Teroson® MS 939-GRP-Araldite Standard-Steel; c) Mounting plate.

exhibits a higher shear strength compared to the primary hyperelastic adhesive to be tested.

The final configurations of the test specimens are illustrated Fig. 3. A mounting plate with shims and spacers was used for the bonding process of the specimens to ensure the position and thickness of the adhesive joints. Four specimens were made for each type, and curing for four weeks was conducted at INESCOP® laboratory room temperature and humidity as mentioned above.

5.5. Digital image analysis

After conducting the tensile shear tests, the surfaces of the specimens were visually analysed, and the percentage of adhesive and cohesive failures was determined. A photo surface analysis method was employed to determine the percentage of adhesive and cohesive failure, as described in Ref. [29]. Using the free ImageJ software, the pixel numbers for the area of cohesive failure and the area of interfacial failure were counted. The pixel numbers were then counted for the area of cohesive failure and the area of interfacial failure using different colours. An example of adhesive failure at 80 % is illustrated in Fig. 4.

6. Results and discussion

6.1. Surface characterization

This section presents the results of contact angles, free surface energy, and roughness for all selected surface treatments. Table 3 provides the average value and standard deviation of the results of the 3 iterations carried out for each type of test.

The contact angles with the two proposed liquids have been measured. Generally, large differences in contact angle between the polar and dispersive liquid have been observed, when comparing with the untreated specimens.

The primed aluminium specimens show a significant reduction in the dispersive angle, of about 50 % compared with the untreated ones. On the contrary, the effect of primer on GRP specimens is not significant.

Regarding the plasma-treated specimens, the results of some aluminium cases trend towards a reduction of around 50 % in both contact angles, polar and dispersive, which translates into higher surface free energy. For GPR specimens the reduction is more significant on polar contact angle. The best results are obtained using low or moderate nozzle velocities and distances. For high velocities and distances, the plasma effect is not effective, approaching the values obtained without treatment.

The sandblasting treatment chosen does not produce significant contact angle variations in the aluminium specimens. For the GRP specimens, sandblasting breaks the material and renders it unusable.

In relation to the roughness measurement, the only treatment that shows a significant effect is the sandblasting of the aluminium samples, which, as expected, produces an increase in roughness. The roughness variations obtained after treatment with plasma are not significant, therefore, it could not be correlated with other studies [30].

6.2. Treatment pre-selection

In view of the contact angle results and the estimated polar affinity of the surface, a number of plasma parameter combinations were pre-selected, to be correlated with SLJ tests in following section. Table 3 represents in bold letter the selected parameters according the next considerations:

For aluminium surfaces: representative configurations with low polar and dispersive angles (AP051-AL), with high polar and dispersive angles (A156-AL), and a configuration with low polar but high dispersive angles (AP109-AL).

For GRP surfaces: representative configurations with very low polar and dispersive angles (AP051-G), with low polar but higher dispersive angle (AP053-G), and two configurations showing moderate polar and dispersive angles (AP101-G with lower polar angle and AP103-G with lower dispersive angle).

In addition, the chemical primer and sandblasting treatments were also a priori selected for the next phase. However, the sandblasted GRP specimens were later finally discarded for SLJ tests, as the polyester surface layer was very deteriorate after the treatment, exposing the fibres. As a consequence, the first SLJ specimens manufactured exhibited

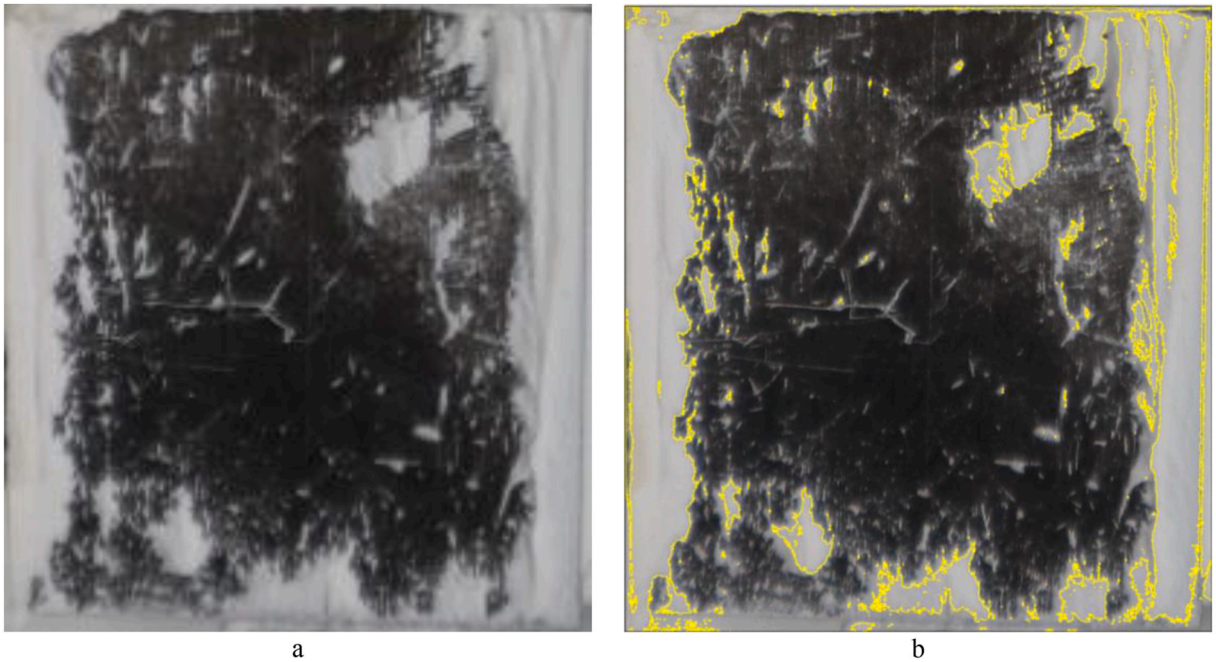

Fig. 4. Example of photo-surface analysis method for the calculation of % adhesivity failed. In a) 1259833 total pixels; b) 1007587 selected pixels. Note: White is adhesive and black is aluminium.

Table 3
Phase 1 contact angle and free surface energy average value results: a) for Aluminium; b) for GRP.

a

	Treatments references	θ_w (°)	θ_d (°)	Y_s (mJ/m^2)	R_a (μm)	R_z (μm)
Without (WT)*(Reference)*	WT-AL	68,55 ± 4,69	43,94 ± 2,06	43,94 ± 2,06	0,35 ± 0,05	0,97 ± 0,19
Sandblasting (SB)	SB-AL	69,65 ± 2,22	45,56 ± 3,89	40,52 ± 0,49	3,66 ± 0,35	21,75 ± 2,29
Primer (PR)	PR-AL	66,55 ± 1,53	27,21 ± 5,68	47,62 ± 0,86	–	–
Sandblasting + Primer (S&P)	S&P-AL	66,73 ± 2,28	27,7 ± 2,22	47,68 ± 0,71	–	–
Atmospheric plasma configurations (AP)	**AP051-AL**	**25,09 ± 4,02**	**26,6 ± 1,21**	**67,1 ± 0,53**	**0,52 ± 0,53**	**1,41 ± 0,23**
	AP053-AL	32,25 ± 6,55	41,22 ± 1	61,84 ± 0,59	–	–
	AP056-AL	27,84 ± 1,34	35,34 ± 1,17	64,99 ± 0,21	–	–
	AP059-AL	27,25 ± 2,59	43,98 ± 2,34	64,47 ± 0,36	–	–
	AP101-AL	25,47 ± 4,35	37,63 ± 2,15	65,75 ± 0,23	–	–
	AP103-AL	37,51 ± 3,49	41,89 ± 1,1	58,99 ± 0,14	–	–
	AP106-AL	34,03 ± 4,73	43,39 ± 1,91	60,75 ± 0,35	–	–
	AP109-AL	**24,12 ± 4,53**	**48,99 ± 1,95**	**65,7 ± 0,53**	**0,32 ± 0,53**	**1,22 ± 0,45**
	AP151-AL	24,26 ± 0,79	45,87 ± 0,48	65,88 ± 0,24	–	–
	AP153-AL	27,56 ± 0,79	51,81 ± 0,48	63,9 ± 0,6	–	–
	AP156-AL	**53,61 ± 2,87**	**57,44 ± 5,7**	**46,46 ± 0,6**	**0,29 ± 0,60**	**1,06 ± 0,22**
	AP159-AL	45,24 ± 1,08	54,68 ± 1,78	52,65 ± 0,73	–	–

b

	Treatment references	θ_w (°)	θ_d (°)	Y_s (mJ/m^2)	R_a (μm)	R_z (μm)
Without (WT) *(Reference)*	WT-G	75,63 ± 2,27	32,27 ± 1,6	43,92 ± 0,43	0,30 ± 0,05	0,84 ± 0,24
Primer (PR)	PR-G	73,61 ± 2,68	32,02 ± 3,16	44,36 ± 0,22	–	–
Atmospheric plasma configurations (AP)	**AP051-G**	**2,47 ± 0,47**	**9,91 ± 1,71**	**73,92 ± 0,03**	**0,36 ± 0,05**	**1,14 ± 0,18**
	AP053-G	**7,32 ± 2,68**	**25,46 ± 0,8**	**72,4 ± 0,7**	**0,26 ± 0,03**	**0,75 ± 0,23**
	AP056-G	5,12 ± 0,98	22,84 ± 2,83	72,91 ± 0,25	–	–
	AP059-G	9,26 ± 1,21	28,67 ± 1,59	71,88 ± 0,22	–	–
	AP101-G	**21,91 ± 2,17**	**30,41 ± 2,17**	**68,05 ± 0,99**	**0,31 ± 0,04**	**0,81 ± 0,07**
	AP103-G	**35,28 ± 1,41**	**28,59 ± 3,64**	**62,12 ± 0,22**	**0,27 ± 0,03**	**0,73 ± 0,14**
	AP106-G	40,26 ± 1,35	34,67 ± 1,47	58,54 ± 0,03	–	–
	AP109-G	39,2 ± 2,7	29,59 ± 2,72	59,64 ± 0,27	–	–
	AP151-G	46,53 ± 1,25	33,61 ± 1,68	55,26 ± 0,8	–	–
	AP153-G	53,73 ± 3,58	38,57 ± 1,72	50,21 ± 1,1	–	–
	AP156-G	68,18 ± 2,7	37,31 ± 2,32	44,01 ± 0,39	–	–
	AP159-G	75,09 ± 1,06	35,94 ± 3,04	42,17 ± 0,58	–	–

(Figure note: θ_w: Polar angle H2O; θ_d: Dispersive angle CH2I2; Y_S: Free surface energy; R_a: Arithmetic mean roughness; R_z: Maximum mean roughness.)

adhesive failure under minimal force, even during manual handling.

6.3. Lap-shear strength tests

This section presents the results of lap-shear strength tests conducted on SLJ specimens. Tables 4 and 5 show the mean value and standard deviation of maximum shear strength, the estimated percentage of the bonded surface showing cohesive/adhesive failure, and a representative image of the broken specimen for each material and treatment considered. The results for aluminium are shown in Table 3, while Table 5 shows the results for the GRP specimens. Once again, the untreated specimens were used as reference.

The untreated aluminium specimens used as a reference (WT-AL) broke at a maximum average strength of 181,2 N/cm^2, producing an 80 % adhesive failure. The GPR specimens used as a reference (WT-G) produced a fully cohesive failure at 220,2 N/cm^2.

The primer-treated specimens (PR-AL and PR-G) had good average strength results (216,9 and 243,0 N/cm^2, respectively) with fully cohesive failure occurring in both cases, and, in the case of the GRP specimens, with a higher average strength.

The sandblasting treatment obtained a high average strength value of 199,8 N/cm^2 in the aluminium specimens (SB-AL) but produced a fully adhesive failure, which is not advisable in structural joints. The mixed sandblasting plus primer treatment on the aluminium specimens (S&P-AL) produced a higher average strength result of 228,5 N/cm^2 than sandblasting alone, with 30 % adhesive failure. Priming compensated for the unfavourable effect of sandblasting to some extent, but the high percentage of adhesive failure still made the failure unpredictable.

The plasma treatments for aluminium (AP051-AL, AP109-AL, and AP156-AL) resulted in mainly cohesive failures, and the average strength results were higher than the untreated ones. The most favourable treatment was AP051-AL, whose value was even above the average strength value for priming.

It was observed that the atmospheric plasma treatment used works best at low speeds and nozzle distances. For aluminium joints with flexible adhesives, plasma treatment can give the same or better results than primer treatment with 100 % cohesive failures, making it a viable alternative to the latter. However, plasma treatment for GRP specimens does not improve the results in any case, making the use of plasma treatments for this material unfeasible.

In conclusion the results obtained for the aluminium substrate show that the SB treatment lead to a higher strength than WT, but its failure mode was fully adhesive. The highest strength result was obtained for the S&P treatment, but it still had a 30 % adhesive failure rate. All plasma specimens showed fully cohesive failure and higher strength values than untreated specimens. The PR and AP051 treatments presented the most desirable results, with 20 % higher strength compared with WT and fully cohesive failures.

In the case of GPR substrate, in contrast to aluminium, no adhesive failure was observed in any of the shear tests conducted on GRP specimens. Consequently, it is not possible to evaluate the positive or negative impact of each treatment on the adhesive bonding capacity of this substrate. In fact, it appears that no plasma surface treatment is required before applying the adhesive to GRP. Plasma treatments seem to negatively influence the maximum shear strength, although further research is needed to investigate this relationship in detail. The AP051 plasma treatment yielded the shear strength value closest to the untreated specimen. Interestingly, despite exhibiting the same type of cohesive failure as the other treatments, the primer treatment demonstrated 10 % highest resistance compared with WT. This may be due to a reduction in surface porosity or chemical changes induced by the primer application, although further research again is needed to investigate this relationship

Table 4
Average of maximum strength and % of failure on aluminium SLJ tests.

SLJ references	Strength, τ (N/cm2)	% failure	Picture example
WT-AL Without (WT) *(Reference)*	181,2 ± 23,9	CF = 20 % AF = 80 %	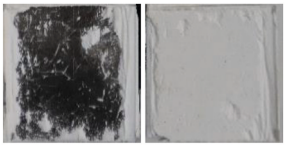
SB-AL Sandblasting (SB)	199,8 ± 29,9	AF = 100 %	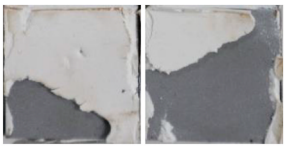
PR-AL Primer (PR)	216,9 ± 15,5	CF = 100 %	
S&P-AL Sandblasting + Primer (S&P)	228,5 ± 11,9	CF = 70 % AF = 30 %	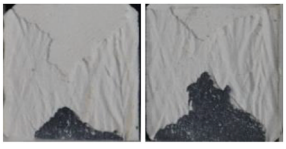
AP051-AL Plasma 1 (AP051)	221,4 ± 9,2	CF = 95 % AF = 5 %	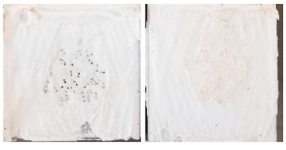
AP109-AL Plasma 2 (AP109)	204,8 ± 5,1	CF = 95 % AF = 5 %	
AP156-AL Plasma 3 (AP156)	199,7 ± 7,5	CF = 95 % AF = 5 %	

Table 5
Average of maximum strength and % of failure on GPR SLJ tests.

SLJ references	Strength, τ (N/cm2)	% failure	Picture example
WT-G Without (WT) *(Reference)*	220,2 ± 18,3	CF = 100 %	
PR-G Primer (PR)	243,0 ± 16,2	CF = 100 %	
AP051-G Plasma 1 (AP051)	213,5 ± 19,8	CF = 100 %	
AP053-G Plasma 2 (AP053)	208,0 ± 3,0	CF = 100 %	
AP101-G Plasma 3 (AP101)	195,9 ± 25,6	CF = 100 %	
AP103-G Plasma 4 (AP103)	193,3 ± 19,0	CF = 100 %	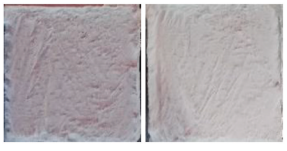

in detail.

6.4. Correlations analysis

This section discusses the comparison between the surface characterisation results and the shear strength results, for the two types of substrate material used.

Contact angle with polar and dispersive liquids, as well as the free surface energy, are presented as indicators of bond strength. Fig. 5 provides a summary of this comparison, showing the results from left to right, in order from the lowest to the highest strength.

Aluminium comparison. Among the aluminium treatments, PR, S&P, and AP051 exhibited the lowest dispersive contact angles. A trend was observed where a lower dispersive contact angle corresponded to higher breaking strength in the plasma-treated samples, with AP051 achieving the highest strength value of them. While both AP051 and AP109 had similar total surface free energy values, AP051's lower dispersive angle contributed to its higher strength. And the primer treatment prevented adhesive failure and increased strength, despite it did not significantly increase surface free energy. And finally, the polar contact angle did not appear to directly influence adhesive strength.

On the other hand, the increase of roughness obtained with the sandblasting treatment, is correlated with a higher shear strength, probably due to a kind of mechanical interactions. However, when finally breaking, and adhesive failure is obtained. A possible explanation for the observed adhesive failure is that increased roughness may lead to micro-tensile stresses in the shear stress direction.

GRP comparison. When comparing the contact angles with the maximum breaking strength, it is evident that the PR treatment exhibited contact angles similar to those of the untreated specimen (WT) but achieved the highest strength value among all treatments. In this case, no clear relationship between improved performance and contact angles could be established. However, when focusing exclusively on plasma treatments, a pattern similar to that observed in aluminium specimens emerged: despite comparable total surface free energy values, lower dispersive angles corresponded to higher breaking strengths. Furthermore, a lower polar angle also appeared to correlate with slight higher breaking strength of the plasma treated specimens, as observed by comparing AP051 with AP053 and AP101.

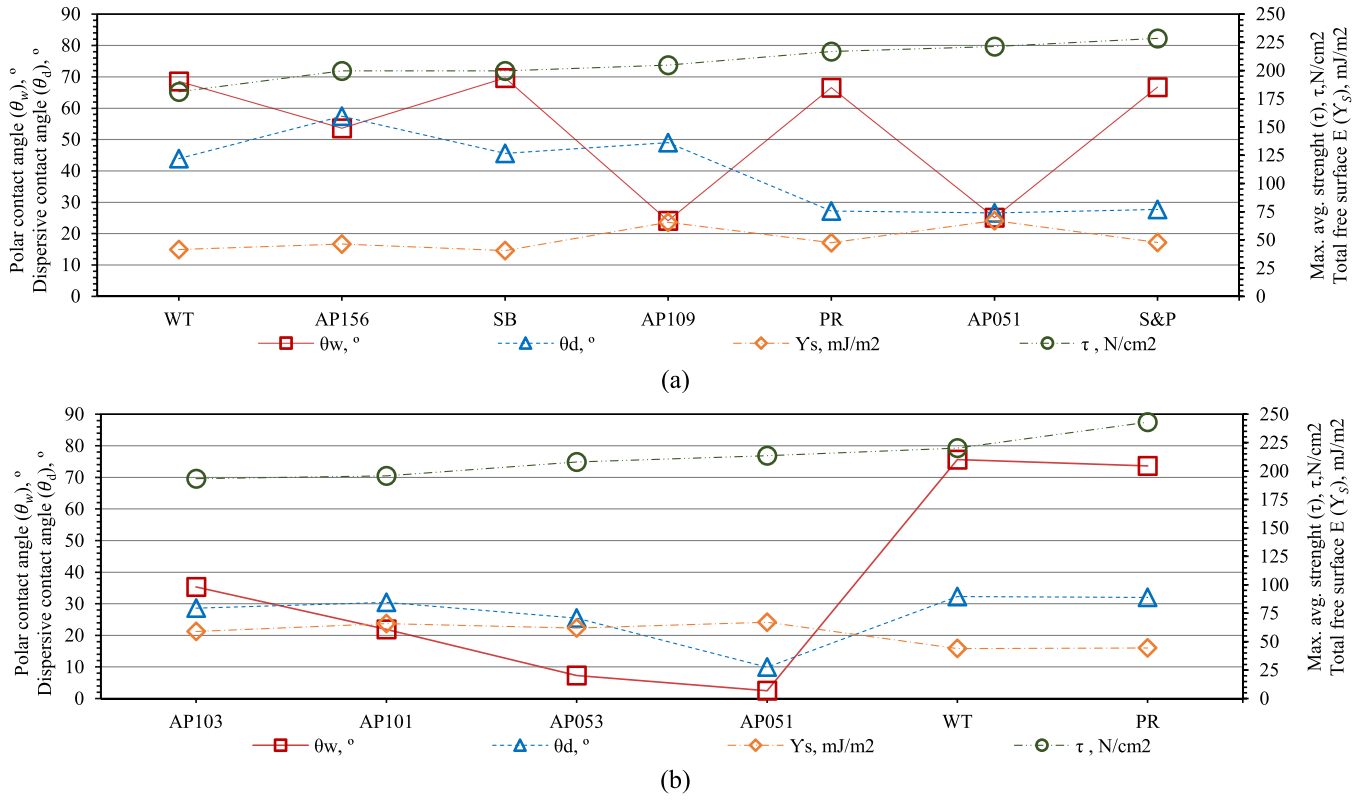

Fig. 5. Comparison results: a) Aluminium, b) GPR.
Figure note: WT: Without treatment, S: Sandblasting, PR: Primer, S&P: Sandblasting and primer, AP: Atmospheric plasma.

6.5. *Adhesive vs substrate affinity*

The relationship observed between the lower dispersive angle and the higher breaking strength, may be due to a possible chemical affinity of the adhesive with the surface. A possible explanation is that the hyperelastic adhesive used may contain a high proportion of dispersive components, which would suggest a greater affinity with the aluminium surface, as indicated by the results obtained.

To further investigate this behaviour, a cured sample of raw SMP adhesive was characterised, looking for the presence of dispersive components. This characterisation was performed by measuring contact angles, calculating surface free energies, and conducting infrared spectroscopy.

Table 6 displays the goniometer results for the cured adhesive. It can be observed that the dispersive contact angle measured on the surface of the cured adhesive sample is significantly lower than that obtained with the polar liquid. Thus, the adhesive surface exhibits a greater affinity towards the dispersive liquid, similar to the substrate surfaces of the stronger bonds.

Fig. 6 shows the Fourier Transform infrared spectrum of the silane modified polymer-based adhesive film used. It illustrates a high aliphatic and silane modified polymer structure. For instance, the bands at 874 cm^{-1} and 1261 cm^{-1} can be attributed to the Si-C stretching symmetric vibration and Si-(CH3) bending symmetric vibration. Additionally, high intensity bands between 2866 and 2968 cm^{-1} and 1425 cm^{-1} can be attributed to CH2 and CH3 aliphatic groups. Therefore, it is expected that a high content of aliphatic groups in the adhesive would interact better with aliphatic moieties on the adherent surface, resulting in a stronger adhesive joint resistance.

On the other hand, despite having dispersive and polar angles very similar to the WT specimens and higher than those obtained with the AP051 plasma treatment, the PR-treated GPR specimens were the most resistant. This suggests that other phenomena may be taking place. The use of a primer on the GRP appears to improve bond strength independently of the surface affinities detected above. A possible explanation for this effect could be the creation of new GPR-SMP bonds resulting from a stronger PU-SMP primer interface. This favourable effect of the introduction of primers has been demonstrated in other studies, such as [19].

7. Conclusions

Results of SLJ tests indicated that plasma treatment on aluminium surfaces increased shear strength values by 20 % compared to untreated surfaces and showed a shear strength comparable to primer application. However, on GRP surfaces, primer application improved bond strength by 10 %, while plasma treatment did not provide any significant enhancement.

Table 6
Goniometer results for cured adhesive.

θ_w (°)	Picture example	θ_d (°)	Picture example	γ_S (mJ /m^2)
72,16 ± 2,03	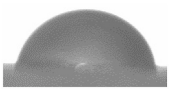	51,13 ± 0,46		37,56 ± 0,62

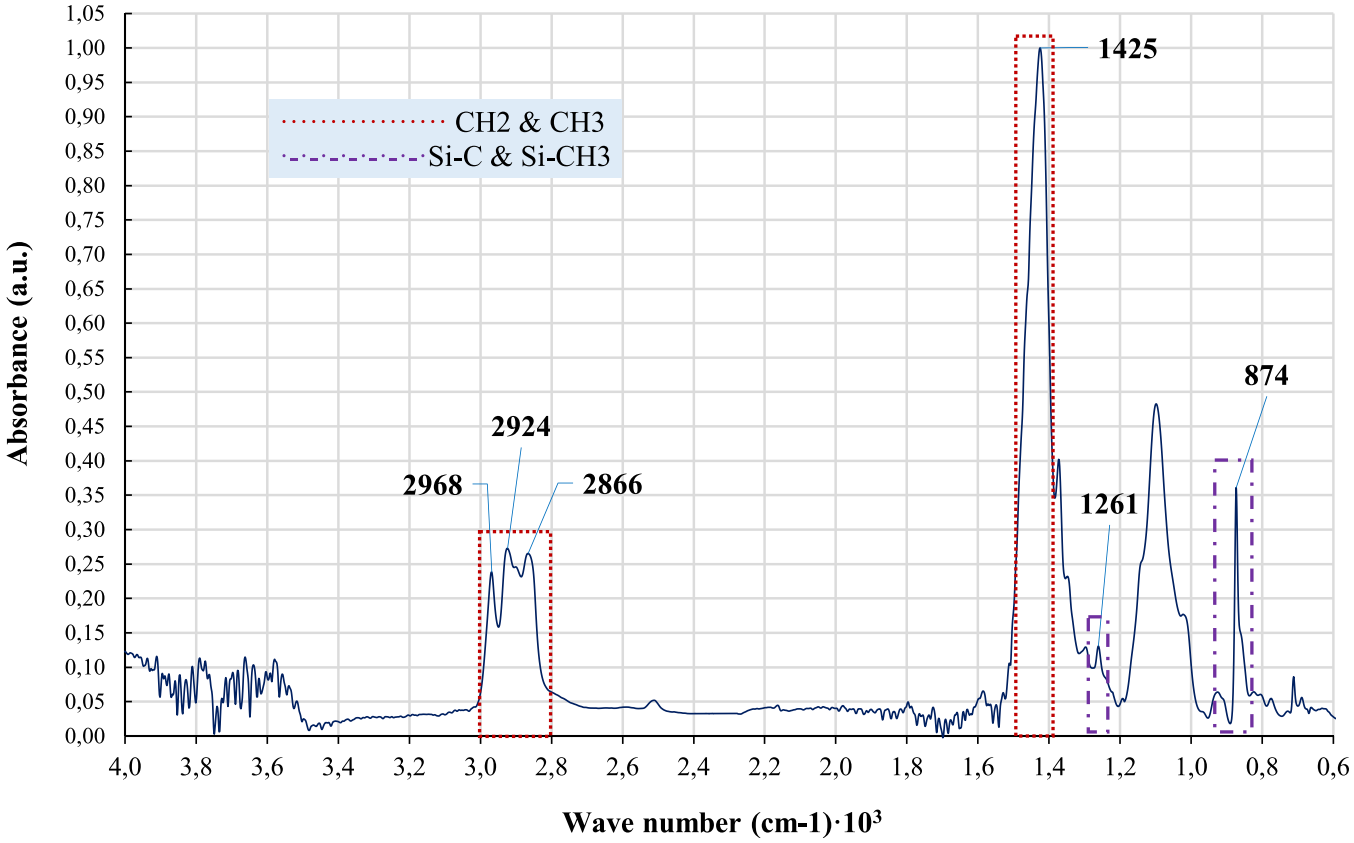

Fig. 6. FTIR spectrum of the adhesive film used.

On the other hand, plasma treatments produce a significant reduction up to 50 % in both polar and dispersive angles on aluminium specimens, and up to 70 % reduction in dispersive contact angle on GRP specimens. The reduction was more pronounced when lower application distance and velocity parameters were used (d_a = 5 mm and v_p = 0,01 m/s). This reduction translates into higher surface free energy.

With respect to joint failure, plasma and primer treatments predominantly resulted in cohesive joint failure (95–100 %). In contrast, sandblasting and sandblasting combined with priming led to a higher incidence of adhesion failure (30–100 %), which is often sudden and unpredictable. These results conclude that plasma treatment can serve as a good alternative to primer on aluminium surfaces, whereas primer application is still preferred for GRP surfaces.

From the correlation of the results above, a relationship arises between the dispersive contact angle and the shear strength of aluminium bonds. In general terms, a 50 % decrease in dispersive contact angle results in a 10 % increase in shear strength. Further investigation of this relationship was carried out, by measuring the polar and dispersive contact angle in a cured specimen of raw adhesive material, and analysing also its FTIR spectrum. The results showed that the dispersive angle (51,13 °) was lower than the polar angle (72,16 °), which would be consistent with the observed higher strength of the bonds with substrates showing also low dispersive angles. The FTIR analysis revealed a high content of aliphatic groups in the adhesive, which would corroborate the affinity detected for the dispersive compounds. These findings are of great interest and justify the continuation of this line of research, to optimise treatments leading to adhesive bonds of improved strength.

CRediT authorship contribution statement

Óscar Cuadrado-Sempere: Conceptualization, Formal analysis, Investigation, Methodology, Writing – original draft, Writing – review & editing. **Francisco-Javier Simón-Portillo:** Investigation, Methodology. **Carlos Ruzafa-Silvestre:** Investigation. **Elena Orgiles-Calpena:** Investigation. **Francisca Arán-Ais:** Investigation, Supervision. **Lucas Filipe Martins da Silva:** Investigation, Supervision. **Miguel Sánchez-Lozano:** Project administration, Supervision, Writing – review & editing.

Declaration of competing interest

The authors declare the following financial interests/personal relationships which may be considered as potential competing interests: The co-autor Lucas Filipe Martins da Silva is actualy member of the Editorial Advisory Boardr of the Journal.

Acknowledgements

This article was supported by funding and technical assistance from the Department of Mechanical Engineering and Energy at Miguel Hernández University of Elche and the INESCOP® Centre for Innovation and Technology. We gratefully acknowledge their support.

Data availability

Data will be made available on request.

References

[1] Liu Y, Du H, Liu L, Leng J. Shape memory polymers and their composites in aerospace applications: a review. Smart Mater Struct 2014;23(2):023001.
[2] Njuguna J, editor. Lightweight composite structures in transport: design, manufacturing, analysis and performance. Woodhead publishing; 2016.
[3] Yancey RN. Challenges, opportunities, and perspectives on lightweight composite structures: aerospace versus automotive. Lightweight composite structures in transport. 2016. p. 35–52.

[4] Mui TSM, Silva LLG, Prysiazhnyi V, Kostov KG. Surface modification of aluminium alloys by atmospheric pressure plasma treatments for enhancement of their adhesion properties. Surf Coating Technol 2017;312:32–6.
[5] Li J, Li Y, Huang M, Xiang Y, Liao Y. Improvement of aluminum lithium alloy adhesion performance based on sandblasting techniques. Int J Adhesion Adhes 2018;84:307–16.
[6] Banea MD, de Queiroz HFM. Application of structural adhesives in composite connections. Structural Adhesives: Properties, Characterization and Applications 2023:375–96.
[7] Das A, Mahanwar P. A brief discussion on advances in polyurethane applications. Advanced Industrial and Engineering Polymer Research 2020;3(3):93–101.
[8] Delavarde A, Savin G, Derkenne P, Boursier M, Morales-Cerrada R, Nottelet B, Caillol S. Sustainable polyurethanes: toward new cutting-edge opportunities. Prog Polym Sci 2024:101805.
[9] Gadhave RV, Gadhave CR, Dhawale PV. Silane terminated prepolymers: an alternative to silicones and polyurethanes. Open J Polym Chem 2021;11(3):31–54.
[10] S. Merenyi. REACH: regulation (EC) No 1907/2006: consolidated version (may 2024) with an introduction and future prospects regarding the area of chemicals legislation.
[11] Bello D, Herrick CA, Smith TJ, Woskie SR, Streicher RP, Cullen MR, et al. Skin exposure to isocyanates: reasons for concern. Environ Health Perspect 2007;115:328–35.
[12] Gupta S, Upadhyaya R. Cancer and p21 protein expression: in relation with isocyanate toxicity in cultured mammalian cells. Int. J. Pharm. Res. Bio-Sci. 2014;3:20–8.
[13] Loginova SE, Gladkikh SN, Kurilova EA, et al. On the possibility of using adhesive–sealants based on MS-polymers for structural glazing. Polym. Sci. Ser. D 2023;16:261–7.
[14] Cornille Adrien, Auvergne Rémi, Figovsky Oleg, Boutevin Bernard, Caillol Sylvain. A perspective approach to sustainable routes for non-isocyanate polyurethanes. Eur Polym J 2017;87:535–52.
[15] da Silva LFM, Öchsner A, Adams RD, editors. Handbook of adhesion technology, vol. 1. Heidelberg: Springer; 2011. p. 1543.
[16] Gent AN. Engineering with rubber: how to design rubber components. Carl Hanser Verlag GmbH Co KG; 2012.
[17] Simón-Portillo FJ, Abellán-López D, Arán F, da Silva LFM, Sánchez-Lozano M. Methodology for the mechanical characterisation of hyperelastic adhesives. Experimental validation on joints of different thicknesses. Polym Test 2023;129:108286.
[18] Critchlow GW, Brewis DM. Review of surface pretreatments for aluminium alloys. Int J Adhesion Adhes 1996;16(4):255–75.
[19] Spaggiari A, Dragoni E. Effect of mechanical surface treatment on the static strength of adhesive lap joints. J Adhes 2013;89(9):677–96.
[20] Saleema N, Sarkar DK, Paynter RW, Gallant D, Eskandarian M. A simple surface treatment and characterization of AA 6061 aluminum alloy surface for adhesive bonding applications. Appl Surf Sci 2012;261:742–8.
[21] Saleema N, Gallant D. Atmospheric pressure plasma oxidation of AA6061-T6 aluminum alloy surface for strong and durable adhesive bonding applications. Appl Surf Sci 2013;282:98–104.
[22] Wu Y, Lin J, Carlson BE, Lu P, Balogh MP, Irish NP, Mei Y. Effect of laser ablation surface treatment on performance of adhesive-bonded aluminium alloys. Surf Coating Technol 2016;304:340–7.
[23] Ruzafa-Silvestre C, Carbonell-Blasco MP, Pérez-Limiñana MA, Arán-Ais F, Orgilés-Calpena E. Robotised atmospheric plasma treatment to improve the adhesion of vulcanised and thermoplastic rubber materials for a more sustainable footwear". Int J Adhesion Adhes 2022;117(Part B):103010.
[24] Pantoja M, Encinas N, Abenojar J, Martínez MA. Effect of tetraethoxysilane coating on the improvement of plasma treated polypropylene adhesion. Appl Surf Sci 2013;280:850–7.
[25] Encinas N, Abenojar J, Martínez MA. Development of improved polypropylene adhesive bonding by abrasion and atmospheric plasma surface modifications. Int J Adhesion Adhes 2012;33:1–6.
[26] Zain NM, Ahmad SH, Ali ES. Effect of surface treatments on the durability of green polyurethane adhesive bonded aluminium alloy. Int J Adhesion Adhes 2014;55:43–55.
[27] Sánchez LM, Cuadrado SO, Navarro AAR, Oliva MMA. Assessment of the influence of surface preparation and adhesive application conditions on the structural behaviour of truck body joints. XIII congress on adhesion and adhesives. 2012. p. 217–27.
[28] Owens DK, Wendt RC. Estimation of the surface free energy of polymers. J Appl Polym Sci 1969;13(8):1741–7.
[29] Kim JG, Choi I, Lee DG. Contact angle and wettability of hybrid surface-treated metal adherends. J Adhes Sci Technol 2013;27(7):794–810.
[30] Rudawska A, Danczak I, Müller M, Valasek P. The effect of sandblasting on surface properties for adhesion. Int J Adhesion Adhes 2016;70:176–90.
[31] Encinas N, Abenojar J, Martínez MA. Development of improved polypropylene adhesive bonding by abrasion and atmospheric plasma surface modifications. Int J Adhesion Adhes 2012;33:1–6.
[32] Kota AK, Kwon G, Tuteja A. The design and applications of superomniphobic surfaces. NPG Asia Mater 2014;6(7). e109-e109.